frontiers | Frontiers in Energy Research

TYPE Original Research
PUBLISHED 08 January 2024
DOI 10.3389/fenrg.2023.1341289

OPEN ACCESS

EDITED BY
Mostafa S. Shadloo,
Institut National des Sciences Appliquées de Rouen, France

REVIEWED BY
Qixiang Hu,
Changzhou Institute of Technology, China
Ce An,
Lanzhou University of Technology, China
Linwei Tan,
Nantong University, China

*CORRESPONDENCE
Xiaogang Ma,
hhdxmxg@126.com

RECEIVED 20 November 2023
ACCEPTED 14 December 2023
PUBLISHED 08 January 2024

CITATION
Ma X, Yang J, Dai T, Wang J, Tang L and Yang Y (2024), Influence of the vertically arranged front injector system on the performance and operational stability of the short jet pump.
Front. Energy Res. 11:1341289.
doi: 10.3389/fenrg.2023.1341289

Influence of the vertically arranged front injector system on the performance and operational stability of the short jet pump

Xiaogang Ma[1]*, Jun Yang[1], Tingting Dai[2], Jun Wang[3], Lei Tang[4,5] and Yang Yang[3]

[1]School of Civil Engineering, North Minzu University, Yinchuan, Ningxia, China, [2]Ningxia Water Resources & Hydropower Survey Design & Research Institute Co., Ltd., Yinchuan, Ningxia, China, [3]College of Animal Science and Technology, Yangzhou University, Yangzhou, Jiangsu, China, [4]Henan Key Laboratory of Water Resources Conservation and Intensive Utilization in Yellow River Basin, North China University of Water Resources and Electric Power, Zhengzhou, Henan, China, [5]College of Water Resources, North China University of Water Resources and Electric Power, Zhengzhou, Henan, China

As the core component of a water conservancy sprinkler irrigation system, the self-priming jet pump is required not only to meet performance criteria for self-priming but also to align with the growing trend toward compactness in sprinkler irrigation systems. This paper takes the short compact self-priming jet pump as the research object whose injector is perpendicular to the main flow direction of the impeller inlet in order to reduce the volume of the jet pump and adopts the method of numerical simulation combined with experimental validation to study the effect of vertical arrangement of the injector on the hydraulic characteristics and operational instability of the self-priming jet pump. The results show that compared with the traditional hydraulic structure, the front injector leads to a significant reduction in the applicable flow range of the short jet pump. The hydraulic efficiency of the jet pump is notably inferior to that of traditional pumps across various flow conditions. This discrepancy arises from the eccentric rotation induced by the front-mounted injector, leading to pronounced circumferential asymmetry in the media flow within the individual impeller channels. Consequently, this asymmetry contributes to increased hydraulic losses in the flow channel. At the same time, the smaller overflow area within the injector enhances the turbulent flow characteristics of the medium, leading to increased instability of the subsequent flow field. This induces the generation of unwieldy low-frequency pressure pulsation signals within the flow channel, which are more readily propagated throughout the sprinkler system. In the practical application of short jet pumps, the circumferentially asymmetric distribution of the media flow in the impeller channel may result in the eccentric rotation of the rotor, thereby diminishing the service life of the pump. Furthermore, the complicated low-frequency signals will induce low-frequency vibration of the hydraulic sprinkler system, reducing the operational stability of the sprinkler system.

KEYWORDS

short-type jet pump, hydraulic performance, instream flow structure, pressure pulsation, unsteady flow

1 Introduction

A jet pump has the characteristics of a simple structure and safe and reliable operation, and it is widely used in the field of water conservancy effuser system and other fields (Xu et al., 2021; Zhang et al., 2022; Winoto et al., 2000). In order to better adapt to the diversity and complexity of the sprinkler irrigation system environment, related scholars have performed many experiments with jet pumps as research objects, with a view to revealing the hydraulic performance and internal flow structure of jet pumps and to provide data support for the application of the pumps in engineering practice (Lu et al., 2015a; Lyu et al., 2016; Aissa et al., 2021). Xu et al. (2022) observed the cavitation phenomenon in jet pumps by means of an experimental system, thus revealing two cavitation mechanisms and properties in jet pumps. Banasiak et al. (2012) conducted performance experiments on the R744 jet pumps which contain different shapes of ejectors and found that the coefficient of performance (COP) is highly dependent on the diffuser length and diameter in the ejector. Furthermore, the structure of the ejector was optimized. Xu et al. (2012) conducted performance experiments on the adjustable ejector with transcriptive CO_2 and analyzed the effect of the pressure at the high-pressure side on the pump system. The results showed that increasing the pressure on the high-pressure side was beneficial in improving the hydraulic characteristics of the pump. Pounds et al. (2013) conducted performance experiments on an injector refrigeration system under different temperature conditions in order to determine the optimum size and installation position of the nozzle. They found that although the ejector refrigeration system can achieve 1.7 times the COP, there will be a problem of critical back pressure. Long et al. (2016) performed performance experiments on a jet pump cavitation reactor at different pressure states. During the limit operation stage, a very violent cavitation phenomenon occurs in the pump, which indicates that the ejector pump has a potential application as a cavitation reactor. Lu et al. (2015b) also conducted performance experiments on a jet pump cavitation reactor at limit state; jet pump operation was also experimentally investigated, and it was found that low flow ratios produce high critical pressure ratios, giving the jet pump a greater ability to cope with the unsteady downstream flow. This provides a reference for jet pumps in realizing automatic dosing control of suction.

With the rapid development of computer technology, numerical simulation has also become one of the important means of academic research (Zhu et al., 2013; Wang et al., 2012a; Zhao et al., 2021). A comparative analysis of shear stress assessment models and Reynolds stress models was conducted by Morrall et al. (2020) The results show that the shear stress transfer analysis has higher accuracy than the Reynolds stress model at high eddy current levels. This improves the theoretical reference for subsequent numerical simulations. Haidl et al. (2021) numerically simulated the hydraulic performance of an ejector in an unstable configuration and safely predicted the minimum gas entrainment for different geometries, orientations, and operating conditions, which provided a theoretical reference for the operation of a conventional liquid–air ejector pump. Shah et al. (2011) numerically simulated a steam jet pump using the direct-contact condensation model in FLUENT to investigate its performance when pumping water using saturated steam. The results show that the mass ratio increases with an increase in steam pressure at constant suction pressure. This provides a theoretical basis for the practical application of jet pumps. Wang et al. (2012b) also used numerical simulation to investigate the internal flow law of steam jet pumps and proposed a wet steam model for transonic flow and found that there is spontaneous condensation when the supersonic flow passes through the nozzle. Kwon et al. (2002) discussed the effect of the mixing chamber shape on the hydraulic characteristics of jet pumps at different jet velocities based on a two-dimensional numerical simulation. The effect of the hydraulic characteristics of the jet pump is discussed, and the optimal mixing chamber structural parameters are derived. Deng et al. (2017) investigated the modified jet pump by numerical simulation and found that self-introduced oscillations cause successive rupture and the formation of liquid–gas interfaces, and the phenomenon is characterized by periodicity. The results of this study help understand the flow pattern within the liquid–air jet pump and, thus, improve the unsteady operation of the pump.

Based on the above study, it was found that although the flow direction of the medium within the traditional jet pump system is the same as that of the impeller inlet medium, there are still problems with its hydraulic performance and operational stability (Saker and Hassan, 2013; Sharifi, 2020; Wang et al., 2019). In order to meet the requirements of limited installation space in engineering practice, a more compact structure, a smaller size of the short section, of the jet pump was proposed (Yang et al., 2023; Yu et al., 2023). The jet pump positions the ejector structure perpendicular to the impeller, significantly reducing the overall footprint of the jet pump. This design is particularly advantageous for adapting to the intricate and variable conditions present in water conservancy sprinkler irrigation environments. However, in cases where the direction of media flow within the jet pump system diverges from that within the impeller, there is a heightened risk of inducing unstable flow within the pump. Therefore, this paper concentrates on a typical short-type jet pump, examining the impact of the vertically oriented injector

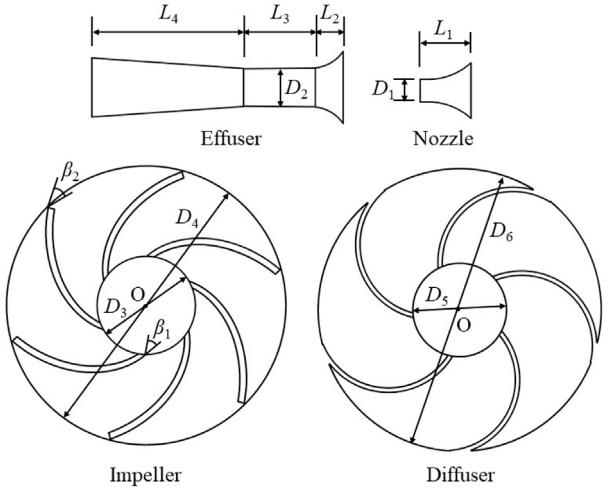

FIGURE 1
Schematic diagram of the main dimensions of a short jet pump.

TABLE 1 Geometric specifications of the impeller and the diffuser.

Nozzle		Impeller	
		Number of blades	$Z = 6$
Nozzle length	L_1 = 22 mm	Inlet diameter	D_3 = 47.5 mm
Outlet diameter	D_1 = 9.2 mm	Outlet diameter	D_4 = 129.5 mm
Effuser		Blade inlet angle	$\beta_1 = 36^\circ$
		Blade outlet angle	$B_2 = 37.5^\circ$
Throat diameter	D_2 = 15 mm	Diffuser	
Inlet area length	L_2 = 12.5 mm	Number of vanes	$Z = 5$
Throat length	L_3 = 25 mm	Inlet diameter	D_5 = 53 mm
Diffuser tube length	L_4 = 62 mm	Outlet diameter	D_6 = 160 mm

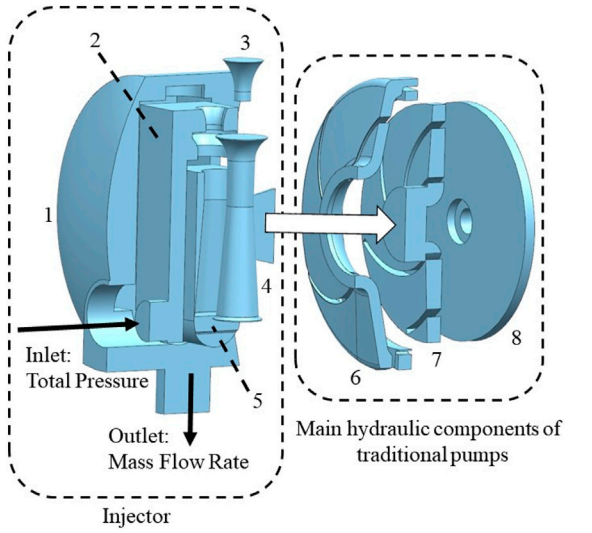

FIGURE 2
3D model of the short-type jet pump.

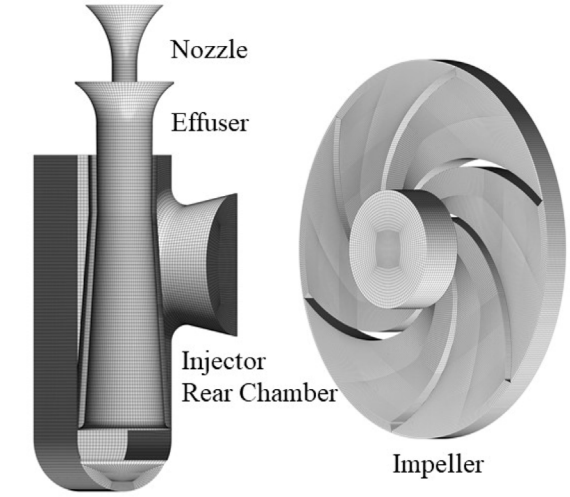

FIGURE 3
Partial computational domain grid of the jet pump.

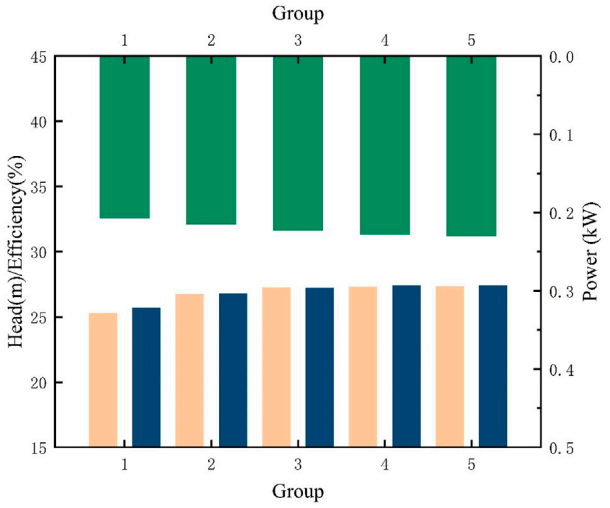

FIGURE 4
Grid irrelevance analysis.

structure on the hydraulic characteristics and internal flow state of the jet pump.

2 Geometry and parameters

This paper adopts a JET1100 short-type jet pump as the research object, which utilizes an effuser to eject the high-pressure medium to form the negative pressure of the jet, so as to suck the air into the nozzle, thus realizing the self-priming function of the pump. The short jet pump mainly includes an effuser, nozzle, impeller, and diffuser and other structures shown in Figure 1, and its main structural parameters are shown in Table 1. Under the rated flow condition, its hydraulic parameters are as follows: a flow rate of 3 m^3/h, head of 28 m, and speed of 2,850 r/min.

3 Numerical simulation

3.1 3D model

This paper employs the "point-line-surface" method for the 3D modeling of the short jet pump, as illustrated in Figure 2. Diverging from the conventional jet pump design, the independent injector structure is vertically fixed at the impeller inlet. This configuration

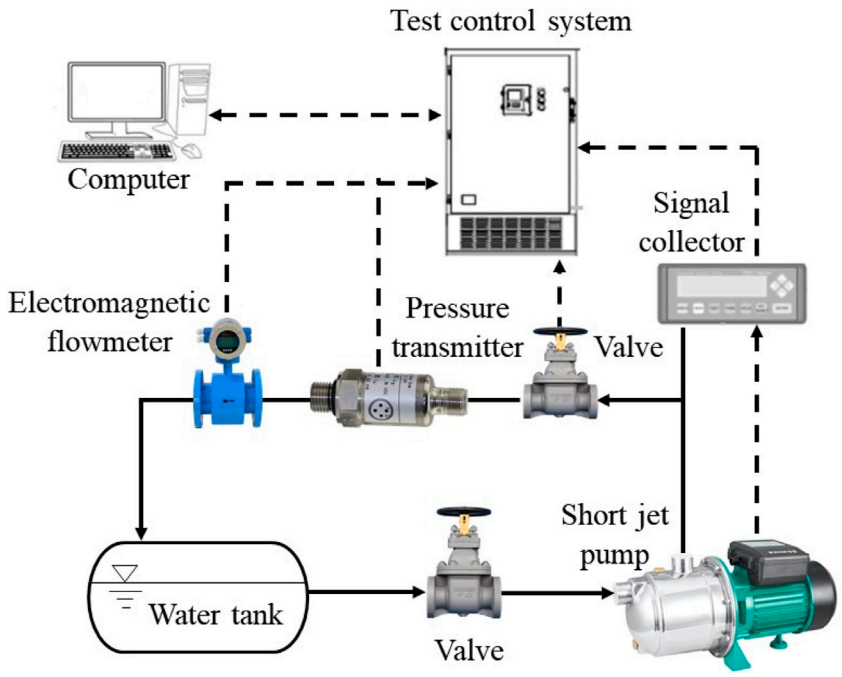

FIGURE 5
Schematic diagram of the test bench.

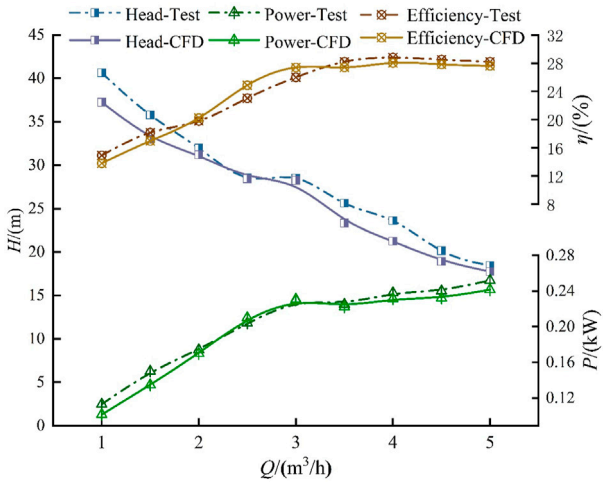

FIGURE 6
Comparison between numerical simulation results and test results.

contributes to the compactness of the jet pump, minimizing its overall size.

3.2 Grid division and irrelevance analysis

In order to improve the efficiency of numerical computation, this paper adopts ICEM software to carry out structured grid delineation of the main overflow components and irrelevance analysis of the mesh number of the impeller and effuser. Part of the computational domain grid is shown in Figure 3. In this paper, five groups of grids are mainly selected for the irrelevance discussion, and the grid numbers are 43,000, 150,000, 442,000, 1,019,000, and 1,473,000. As depicted in Figure 4, an increase in the number of grids results in a gradual reduction in the magnitude of changes observed in head, efficiency, and power. Specifically, when the number of grids reaches 1.019 million in group 4, the growth rate in head, efficiency, and power is less than 0.1%. This suggests that the number of grids in group 4 is economically viable. Consequently, all subsequent numerical simulations in this paper will employ the grid size of group 4.

3.3 Boundary condition setting

In this paper, ANSYS CFX software is used to numerically simulate the computational domain. Pressure inlet with a mass flow outlet is used. The impeller is set as the rotating domain, and other parts are set as the stationary domain. All the intersection interfaces are connected by GGI. Among them, the cross-interface related to the impeller is set as the frozen rotor, and the other cross-interfaces are set as general connection. The residual of the control equation is set as 10^{-4}. For the non-stationary calculation, it is chosen to calculate one step for every 3° rotation of the impeller and 20 iterations for each step. Therefore, the set time step is 1.75×10^{-4}, and the total time is 0.168 s. The standard k-ε turbulence model is used for both stationary and non-stationary calculations in this paper.

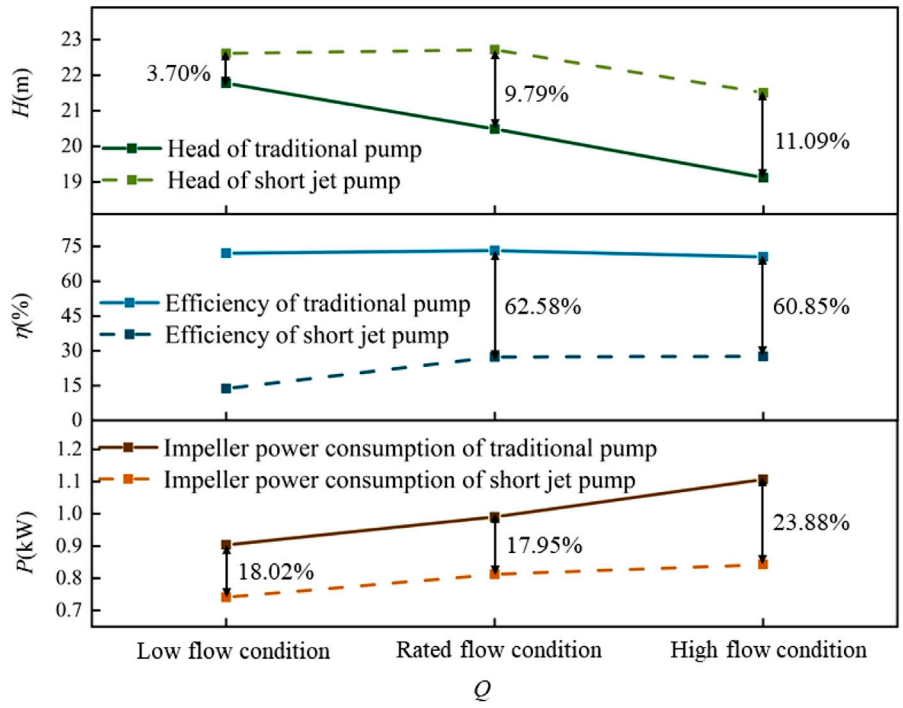

FIGURE 7
Comparison of the hydraulic performance of the two pump types under different flow conditions.

The turbulent kinetic energy k and dissipation rate equations are shown as follows:

$$\frac{\partial(\rho k)}{\partial t} + \nabla \cdot (\rho U k) = \nabla \cdot \left[\left(\mu + \frac{\mu_t}{\sigma_k}\right)\nabla k\right] + P_k + P_b - \rho\varepsilon + S_k, \quad (1)$$

$$\frac{\partial(\rho\varepsilon)}{\partial t} + \nabla \cdot (\rho U \varepsilon) = \nabla \cdot \left[\left(\mu + \frac{\mu_t}{\sigma_\varepsilon}\right)\nabla \varepsilon\right] + C_1 \frac{\varepsilon}{K}(P_k + C_3 G_b) - C_2 \rho \frac{\varepsilon^2}{k} + S_\varepsilon, \quad (2)$$

where P_k is the turbulent kinetic energy generated by the mean velocity gradient (J); P_b indicates the turbulence kinetic energy generated by buoyancy (J); σ_k and σ_ε are the Prandtl numbers of k and ε, respectively; S_k and S_ε are user-defined; C_1, C_2, C_3, and C_μ are constants; and μ_t is the turbulent viscosity (mPa-s).

Unlike other turbulence models, the damping function is used in the ANSYS CFD solver, which enables more accurate prediction of the turbulent motion near the wall. Furthermore, the standard k–ε turbulence model is economical and robust (Launder and Sharma, 1974; Launder and Spalding, 1983).

4 Test verification

In order to verify the accuracy of the numerical simulation results in this paper, a performance test was conducted on the short-type jet pump, and the test process is shown in Figure 5. As shown in the figure, when the short-type jet self-priming pump is running, the pressure transmitter and electromagnetic flow meter are used to monitor and record the pressure and flow data of the test process, respectively. The sensors transmit the collected data to the test control system, and the computer connected to the control system processes the data and provides real-time feedback.

The comparison between the numerical simulation results and the test results for different flow conditions is shown in Figure 6. As shown in the figure, the experimental and numerical simulation values of efficiency and power increase with the increase in the flow rate, while the experimental and numerical simulation values of head decrease with the increase in the flow rate. At full flow conditions, both results have the same trend. In the off-rated flow conditions, the head and power test results and numerical simulation results deviate more. This is due to the fact that the jet pump contains an independent injector structure, which enhances the transient characteristics of the pump, and the steady-state numerical simulation results cannot better capture the transient changes in pump performance. Nevertheless, at the rated flow condition, the numerical simulation results for head, efficiency, and power exhibit a marginal variance of only 0.9%, 1.2%, and 0.3%, respectively, when compared to their corresponding experimental results. This indicates that the numerical simulation method used in this study demonstrates a high level of accuracy.

5 Analysis of results

Figure 7 shows a comparison of the hydraulic performance of the short jet pump and the traditional pump (without a built-in ejector) under different flow conditions. As shown in the figure, with the increase in the flow rate, the head of both the traditional pump and the short jet pump gradually decreased, and the impeller power

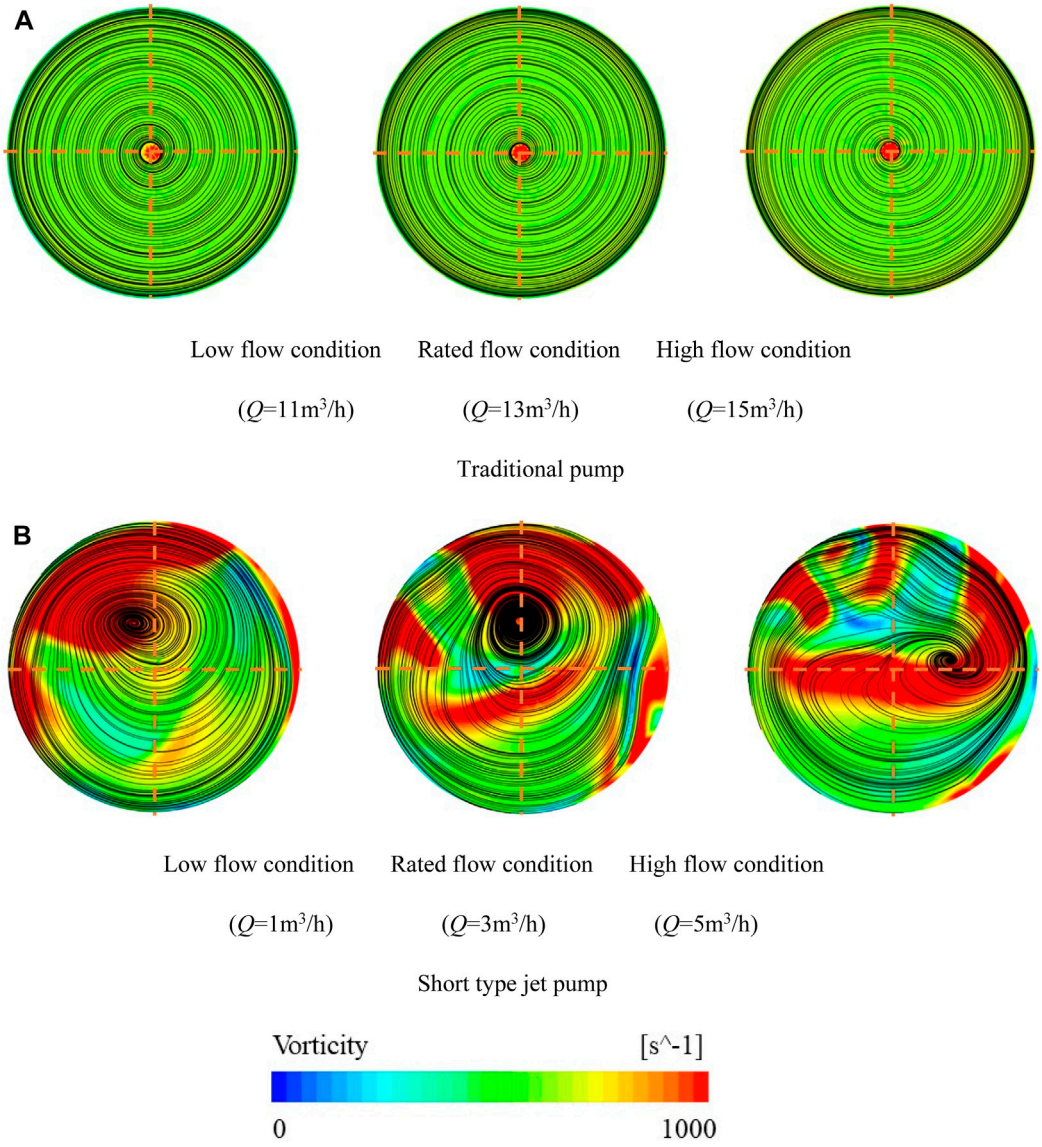

FIGURE 8
Comparison of the vorticity distribution at the inlet of the two pump impellers under different flow conditions.

consumption of the two increased. However, in the same flow conditions, the hydraulic performance of the two shows a noticeable gap. Specifically, in low-flow conditions, the impeller power consumption and efficiency of the short jet pump are lower than those of the traditional pump. Notably, the pump efficiency exhibits a substantial difference, reaching 80.84%. Conversely, the head of the short jet pump under low-flow conditions is significantly higher than that of the traditional pump, with a difference of 3.70%. In the high-flow conditions, the efficiency of the short jet pump and impeller power consumption are also lower than those of the traditional pump, but the difference between the two is relatively small. At this time, the difference in the efficiency and impeller power consumption is 60.85% and 23.88%, respectively, but the jet pump head is still greater than the traditional pump head, and the difference between the two is 11.09%. Under rated flow conditions, while the head of the short jet pump surpasses that of the traditional pump by 3.3%, there persists a noticeable gap in efficiency and impeller power consumption between the two. This observation suggests that despite the short jet pump's ability to suction media to a certain height, the presence of the front injector induces varying flow directions within the pump, potentially leading to unstable flow. Consequently, this may significantly decrease the energy conversion rate of the jet pump.

A comparison of the vorticity distribution of the impeller inlet of the short jet pump and the conventional pump for different flow conditions is shown in Figure 8. As shown in the figure, the addition of jets in the pump leads to a great reduction in the value of the rated flow rate. In this paper, the rated flow rate of the traditional pump is $Q = 13\ m^3/h$, while the rated flow rate of the jet pump is $Q = 3\ m^3/h$. For the traditional pump, there is only high vortex at the center of the impeller inlet in the three flow conditions, and the vortex distribution around the pump is

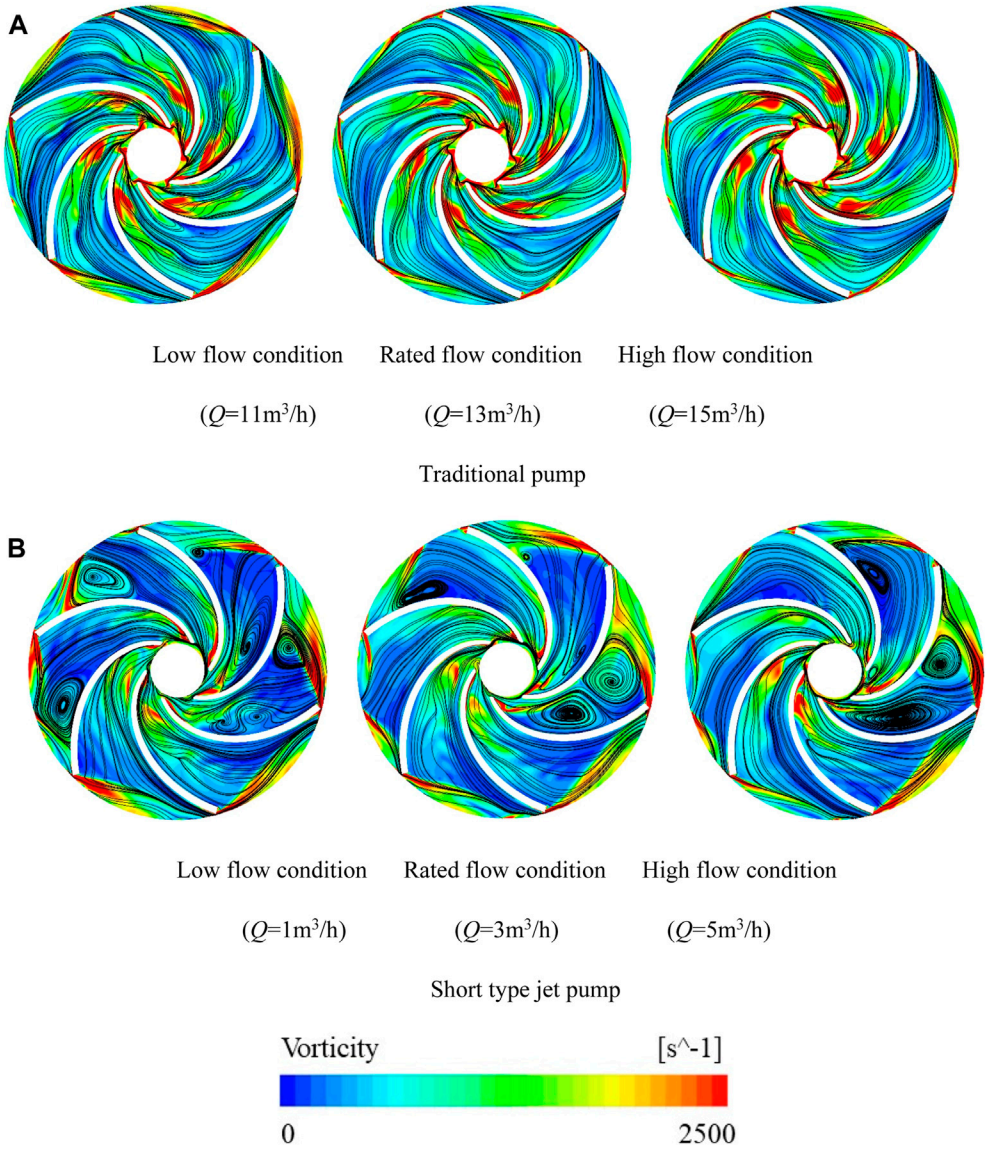

FIGURE 9
Comparison of the impeller mid-span vortex distribution for the two pump types under different flow conditions.

relatively uniform. As the flow rate increases, the traditional pump impeller inlet high-vortex area has to expand outward performance, but the change is not noticeable. However, in different flow conditions, there is a wide range of high-vortex phenomena within the short type of the jet pump. This suggests that, during this period, the energy loss in the pump is more pronounced, resulting in lower pump efficiency, aligning with the previously discussed results. Simultaneously, a comparison of the speed distribution in the two pump types reveals that the traditional pump's impeller inlet vortex exhibits a generally centrosymmetric distribution. In contrast, the vortex inside the short jet pump displays varying degrees of eccentricity. As the flow rate increases, the center of the vortex inside the jet pump gradually moves from the left to the right. This indicates that the front-end transverse jet will lead to the mainstream direction, and the impeller inlet surface normal direction is not consistent, resulting in an uneven distribution of the media at the impeller inlet, thus generating an asymmetric vortex phenomenon.

A comparison of the vorticity distribution at the impeller mid-span of the conventional pump and the short jet pump for three flow conditions is shown in Figure 9. As shown in the figure, the phenomenon of high vorticity occurs at this position in the conventional pump under different flow conditions. The high vortex region is mainly distributed in the blade root and blade tip. At this time, the distribution position of the high-vortex phenomenon at the impeller mid-span in the jet pump is the same as that of the traditional pump, but its distribution range is noticeably larger. In addition, by observing the velocity streamline distribution, it can be found that the streamline shapes in the six impeller channels of the short jet pump are different. Some of the streamlines are uniformly distributed within the flow channels, but single or even multiple vortices appear in some of the flow channels. The range of vortices within the impeller channels is relatively

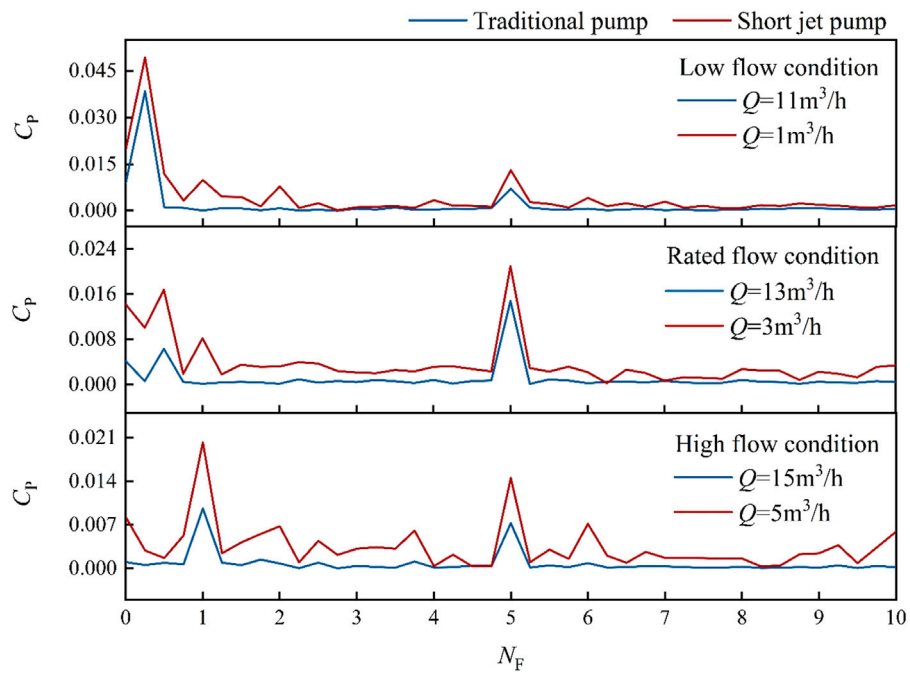

FIGURE 10
Comparison of the pressure pulsation characteristics of the two pump types under different flow conditions.

small under rated flow conditions. This is most likely influenced by the asymmetric distribution of the impeller inlet vortex. Eccentric rotation of the impeller inlet medium induces subsequent flow inconsistencies in each flow channel, which may lead to the presence of large radial forces in the impeller, causing the impeller to rotate eccentrically. The long-term eccentric rotation will cause serious wear and tear of the pump shaft, shortening the service life of the pump.

In order to facilitate the comparison of the pressure pulsation characteristics between traditional pumps and short-type jet pumps, the frequency of the two is converted into a multiple of the impeller rotation frequency, and the rotation frequency multiple N_F is defined as follows:

$$N_F = \frac{60f}{n}, \tag{3}$$

where n represents the rotational speed of the impeller, r/min; f represents the frequency obtained after the fast Fourier transform, Hz.

Figure 10 shows a comparison of the pressure pulsation characteristics at the impeller channel in the two pumps under three flow conditions. Under small flow conditions, the primary frequency in the impeller channel of traditional pumps and short-type jet pumps is distributed in the vicinity of 0.5 times the frequency of rotation, and the secondary frequency is distributed in the vicinity of 5 times the frequency of rotation (diffuser frequency). However, the jet pump also exhibits numerous multi-frequency signals, indicating that the media pressure within the short-type jet pump impeller channel is not only influenced by the impeller and diffuser but also significantly affected by the injector. Under rated flow conditions, the primary frequency of both pumps is concentrated at the diffuser lobe frequency. Additionally, as the frequency increases, the amplitude of pressure pulsations decreases. This phenomenon can be attributed to media fluctuations during the flow process, consequently impacting the pressure distribution in the impeller channel. Moreover, under high-flow conditions, the primary frequency of both pumps is distributed around one times rpm and five times rpm. Compared with the pressure pulsation intensity of conventional pumps, the pressure pulsation amplitude of the jet pump is intense and more frequent. This indicates that the small overflow area at the nozzle and effuser throat will significantly strengthen the turbulent flow characteristics of the medium here, which induces the instability of the subsequent flow field, and the pressure pulsation signal caused by the unstable flow in the flow field will be propagated to the impeller and the diffuser in the flow channel. This characteristic is further amplified under high-flow conditions, thus showing a noticeable pressure fluctuation phenomenon.

6 Conclusion

In this paper, a combination of numerical simulation and experimental verification is used to compare the hydraulic characteristics, internal flow structure, and pressure pulsation characteristics of the JET1100 short-type jet pump with the corresponding conventional pump. The main conclusions are as follows:

(1) Compared with the conventional pump, the rated flow value of the short-type jet pump is significantly lower. Through the comparison of the three different flow conditions of the hydraulic performance of the short-type jet pump and the traditional pump, it was found that the difference between the two heads is small, and the head value of the jet pump is higher than that of the traditional pump. However, the

efficiency of the jet pump is much smaller than the efficiency of the traditional pump. This shows that in the same flow conditions, the short-type jet pump will lose more energy.

(2) Based on the comparison of the flow structure of the two pumps, the front injector will lead to the direction of the medium in the pump, different from the impeller inlet normal direction, which leads to the eccentric rotation of the impeller inlet medium, leading to the phenomenon of unstable flow in the pump. At the same time, the eccentric rotation of the impeller inlet will also induce the subsequent flow inconsistency of each flow channel of the impeller, which will lead to the eccentric rotation of the impeller and reduce the service life of the pump.

(3) By comparing the pressure pulsation characteristics of the two pumps, the narrow overflow area in the injector enhances the turbulent flow characteristics of the medium and induces the instability of the subsequent flow field, which leads to a wide range of low-frequency signals in the pump. This suggests that short-type jet pumps may have low-frequency vibration problems in engineering applications, thus affecting the operational stability of hydraulic sprinkler irrigation systems.

Data availability statement

The original contributions presented in the study are included in the article/Supplementary Material; further inquiries can be directed to the corresponding author.

Author contributions

XM: conceptualization, formal analysis, and writing–review and editing. JY: methodology and writing–original draft. TD: conceptualization and writing–original draft. JW: methodology and writing–review and editing. LT: software and writing–review and editing. YY: supervision and writing–review and editing.

Funding

The authors declare financial support was received for the research, authorship, and/or publication of this article. This work was supported by the Natural Science Foundation of Ningxia Province of China (No. 2021AAC03188), the Ningxia Hui Autonomous Region Key R&D Projects (No. 2021BEG02012), and the General Scientific Research Project of North Minzu University (No. 2021XYZTM06).

Conflict of interest

Author TD was employed by Ningxia Water Resources and Hydropower Survey Design and Research Institute Co., Ltd.

The remaining authors declare that the research was conducted in the absence of any commercial or financial relationships that could be construed as a potential conflict of interest.

Publisher's note

References

Aissa, W. A., Eissa, M. S., and Mohamed, A. H. H. (2021). Experimental and theoretical investigation of water jet pump performance. *Int. J. Appl. Energy Syst.* 3 (1), 1–14. doi:10.21608/ijaes.2021.169900

Banasiak, K., Hafner, A., and Andresen, T. (2012). Experimental and numerical investigation of the influence of the two-phase ejector geometry on the performance of the R744 heat pump. *Int. J. Refrig.* 35 (6), 1617–1625. doi:10.1016/j.ijrefrig.2012.04.012

Deng, X., Dong, J., Wang, Z., and Tu, J. (2017). Numerical analysis of an annular water–air jet pump with self-induced oscillation mixing chamber. *J. Comput. Multiph. Flows* 9 (1), 47–53. doi:10.1177/1757482X16688476

Haidl, J., Mařík, K., Moucha, T., Rejl, F. J., Valenz, L., and Zednikova, M. (2021). Hydraulic characteristics of liquid–gas ejector pump with a coherent liquid jet. *Chem. Eng. Res. Des.* 168, 435–442. doi:10.1016/j.cherd.2021.02.022

Kwon, O. B., Kim, M. K., Kwon, H. C., and Bae, D. S. (2002). Two-dimensional numerical simulations on the performance of an annular jet pump. *J. Vis.* 5, 21–28. doi:10.1007/bf03182599

Launder, B. E., and Sharma, B. I. (1974). Application of the energy-dissipation model of turbulence to the calculation of flow near a spinning disc. *Lett. heat mass Transf.* 1 (2), 131–137. doi:10.1016/0094-4548(74)90150-7

Launder, B. E., and Spalding, D. B. (1983). The numerical computation of turbulent flows. *Comput. Methods Appl. Mech. Eng.* 3, 269–289. doi:10.1016/0045-7825(74)90029-2

Long, X., Zhang, J., Wang, Q., Xiao, L., Xu, M., Lyu, Q., et al. (2016). Experimental investigation on the performance of jet pump cavitation reactor at different area ratios. *Exp. Therm. Fluid Sci.* 78, 309–321. doi:10.1016/j.expthermflusci.2016.06.018

Lu, X., Wang, D., Shen, W., and Zhu, C. (2015a). Experimental investigation of the propagation characteristics of an interface wave in a jet pump under cavitation condition. *Exp. Therm. Fluid Sci.* 63, 74–83. doi:10.1016/j.expthermflusci.2015.01.008

Lu, X., Wang, D., Shen, W., Zhu, C., and Qi, G. (2015b). Experimental investigation on liquid absorption of jet pump under operating limits. *Vacuum* 114, 33–40. doi:10.1016/j.vacuum.2015.01.004

Lyu, Q., Xiao, Z., Zeng, Q., Xiao, L., and Long, X. (2016). Implementation of design of experiment for structural optimization of annular jet pumps. *J. Mech. Sci. Technol.* 30, 585–592. doi:10.1007/s12206-016-0112-y

Morrall, A., Quayle, S., and Campobasso, M. S. (2020). Turbulence modelling for RANS CFD analyses of multi-nozzle annular jet pump swirling flows. *Int. J. Heat Fluid Flow* 85, 108652. doi:10.1016/j.ijheatfluidflow.2020.108652

Pounds, D. A., Dong, J. M., Cheng, P., and Ma, H. B. (2013). Experimental investigation and theoretical analysis of an ejector refrigeration system. *Int. J. Therm. Sci.* 67, 200–209. doi:10.1016/j.ijthermalsci.2012.11.001

Saker, A. A., and Hassan, H. Z. (2013). Study of the different factors that influence jet pump performance. *Open J. Fluid Dyn.* 3 (2), 44–49. doi:10.4236/ojfd.2013.32006

Shah, A., Chughtai, I. R., and Inayat, M. H. (2011). Experimental and numerical analysis of steam jet pump. *Int. J. Multiph. flow* 37 (10), 1305–1314. doi:10.1016/j.ijmultiphaseflow.2011.07.008

Sharifi, N. (2020). Numerical study of non-equilibrium condensing supersonic steam flow in a jet-pump based on supersaturation theory. *Int. J. Mech. Sci.* 165, 105221. doi:10.1016/j.ijmecsci.2019.105221

Wang, J., Cheng, H., Xu, S., Ji, B., and Long, X. (2019). Performance of cavitation flow and its induced noise of different jet pump cavitation reactors. *Ultrason. Sonochemistry* 55, 322–331. doi:10.1016/j.ultsonch.2019.01.011

Wang, X. D., Dong, J. L., Wang, T., and Tu, J. Y. (2012a). Numerical analysis of spontaneously condensing phenomena in nozzle of steam-jet vacuum pump. *Vacuum* 86 (7), 861–866. doi:10.1016/j.vacuum.2011.02.016

Wang, X. D., Lei, H. J., Dong, J. L., and Tu, J. Y. (2012b). The spontaneously condensing phenomena in a steam-jet pump and its influence on the numerical simulation accuracy. *Int. J. heat mass Transf.* 55 (17-18), 4682–4687. doi:10.1016/j.ijheatmasstransfer.2012.04.028

Winoto, S. H., Li, H., and Shah, D. A. (2000). Efficiency of jet pumps. *J. Hydraulic Eng.* 126 (2), 150–156. doi:10.1061/(ASCE)0733-9429(2000126:2(150)

Xu, K., Wang, G., Zhang, L., Wang, L., Yun, F., Sun, W., et al. (2021). Multi-objective optimization of jet pump based on RBF neural network model. *J. Mar. Sci. Eng.* 9 (2), 236. doi:10.3390/jmse9020236

Xu, S., Wang, J., Cai, B., Cheng, H., Ji, B., Zhang, Z., et al. (2022). Investigation on cavitation initiation in jet pump cavitation reactors with special emphasis on two mechanisms of cavitation initiation. *Phys. Fluids* 34 (1). doi:10.1063/5.0075099

Xu, X. X., Chen, G. M., Tang, L. M., and Zhu, Z. J. (2012). Experimental investigation on performance of transcritical CO2 heat pump system with ejector under optimum high-side pressure. *Energy* 44 (1), 870–877. doi:10.1016/j.energy.2012.04.062

Yang, Y., Wu, S., Wang, C., Jiao, W., Ji, L., An, C., et al. (2023). Effect of effuser throat diameter on the internal flow structure and energy characteristics of the jet pump. *Energy Rep.* 9, 2075–2086. doi:10.1016/j.egyr.2023.01.025

Yu, H., Wang, C., Li, G., Wang, H., Yang, Y., Wu, S., et al. (2023). Steady and unsteady flow characteristics inside short jet self-priming pump. *Sustainability* 15 (18), 13643. doi:10.3390/su151813643

Zhang, H., Zou, D., Yang, X., Mou, J., Zhou, Q., and Xu, M. (2022). Liquid–gas jet pump: a review. *Energies* 15 (19), 6978. doi:10.3390/en15196978

Zhao, G., Liang, N., Zhang, Y., Cao, L., and Wu, D. (2021). Dynamic behaviors of blade cavitation in a water jet pump with inlet guide vanes: effects of inflow non-uniformity and unsteadiness. *Appl. Ocean Res.* 117, 102889. doi:10.1016/j.apor.2021.102889

Zhu, F. N., Liu, D., Yang, X. Y., and Wang, C. L. (2013). Numerical simulation of the three-dimensional turbulent flow in roto-jet pump. *Appl. Mech. Mater.* 341, 375–378. doi:10.4028/www.scientific.net/AMM.341-342.375